Welding International

ISSN: (Print) (Online) Journal homepage: www.tandfonline.com/journals/twld20

Influence of dwell time on microstructure and mechanical properties of Friction Stir Spot welded aluminium dissimilar joints

Suresh S, Balaji J, Elango Natarajan, Velmurugan D & Elayaraja R

To cite this article: Suresh S, Balaji J, Elango Natarajan, Velmurugan D & Elayaraja R (04 Feb 2025): Influence of dwell time on microstructure and mechanical properties of Friction Stir Spot welded aluminium dissimilar joints, Welding International, DOI: 10.1080/09507116.2025.2460533

To link to this article: https://doi.org/10.1080/09507116.2025.2460533

WELDING INTERNATIONAL
https://doi.org/10.1080/09507116.2025.2460533

Taylor & Francis
Taylor & Francis Group

RESEARCH ARTICLES

Influence of dwell time on microstructure and mechanical properties of Friction Stir Spot welded aluminium dissimilar joints

Suresh S[a], Balaji J[a], Elango Natarajan[b], Velmurugan D[c] and Elayaraja R[d]

[a]Department of Mechanical Engineering, Erode Sengunthar Engineering College, Erode, India; [b]Faculty of Engineering, Technology and Built Environment, UCSI University, Kuala Lumpur, Malaysia; [c]Department of Mechanical Engineering, Muthayammal Engineering College, Rasipuram, India; [d]School of Mechanical Engineering, Vellore Institute of Technology, Vellore, India

ABSTRACT

This research investigates the effect of dwell time on the microstructural and mechanical properties of friction stir spot welded (FSSW) dissimilar joints between AA6061 and AA7075 aluminium alloys, with implications for automotive, aerospace, and structural applications. FSSW was performed on 2 mm thick plates with varying dwell times (2 to 8 s), and the resulting joints were analysed for weld quality using macrographs, microstructure evaluations, and mechanical testing under room temperature conditions. Notably, a 6-second dwell time achieved the maximum lap shear fracture load of 5925 N, attributed to optimised heat input and material flow. However, increasing the dwell time to 8 s led to decreased joint strength due to excessive heat, which affected grain structure and bond integrity. Fracture surfaces examined *via* Field Emission Scanning Electron Microscopy (FESEM) provided insights into the failure mechanisms associated with each dwell time. These findings underscore the importance of dwell time optimisation in maximizing joint performance for high-strength dissimilar aluminium alloy applications.

ARTICLE HISTORY
Received 5 December 2024
Accepted 12 January 2025

KEYWORDS
AA6061; AA7075; friction stir spot welding; dwell time; lap shear fracture load

1. Introduction

In recent years, the demand for lightweight and high-strength materials has surged, particularly in industries such as automotive, aerospace, and construction, where reducing weight without compromising performance is critical. Aluminium alloys, especially 6XXX and 7XXX, have emerged as leading candidates due to their exceptional strength-to-weight ratio, corrosion resistance, and versatility [1, 2]. AA6061 and AA7075 are widely used in industries such as automotive and aerospace due to their high strength-to-weight ratios and superior corrosion resistance. While AA6061 is known for its excellent weldability, moderate strength, and good thermal properties, AA7075 offers superior mechanical strength and fatigue resistance but presents challenges in welding due to its susceptibility to thermal cracking and loss of strength at weld zones. The combination of these alloys in dissimilar joints enables the utilization of their complementary properties. The dissimilar joints are increasingly relevant in applications requiring lightweight structures with differential performance requirements, such as automotive chassis, aerospace components, and structural applications [3–5]. However, welding dissimilar aluminium alloys presents unique challenges due to differences in their thermal and mechanical properties. Traditional fusion welding methods can introduce defects such as porosity and cracks, weakening the joints [6, 7]. To overcome these limitations, friction-based solid-state welding techniques, such as Friction Stir Spot Welding (FSSW), are employed [8–10]. FSSW, initially developed from Friction Stir Welding (FSW) and first adopted by Mazda in 1993, offers advantages like high joint efficiency, minimal distortion, and lower costs [11–13]. Unlike conventional welding, FSSW creates spot welds by generating frictional heat through a rotating tool that stirs and bonds the overlapping metal sheets [14–16].

FSSW has gained significant attention from researchers due to its advantages over current

CONTACT Elango Natarajan cad.elango.n@gmail.com Faculty of Engineering, Technology and Built Environment, UCSI University, Kuala Lumpur, Malaysia.

spot joining methods, including high joint efficiency, low joint distortion, cost-effectiveness, a clean working environment, and the ability to weld a range of materials without requiring filler material [17, 18]. Among the key process parameters influencing joint quality are tool rotational speed, plunge rate, and dwell time. Dwell time, which dictates how long the tool remains in contact with the workpiece, plays a critical role in determining the heat input and material flow during welding [19, 20]. Although several studies have investigated the impact of these parameters, limited research focuses specifically on the effects of dwell time on fracture load and mechanical properties of dissimilar aluminium alloy joints [21–23].

The tool geometry affects the welded structure and material flow in FSSW, influencing hook dimensions, stir zone width, and joint performance, with dwell time and tool rotation speed being key parameters in heat generation and weld quality [24, 25]. Choi et al. [26] experimented using a high-strength steel tool with a shoulder, shank, and probe to join Al/Mg alloys. They observed the formation of intermetallic compounds (IMCs) at the interface. By increasing the tool's rotational speed and holding time, the IMC layer thickened significantly, which notably affected the joint strength. Zhang et al. [27] explored how varying tool rotational speeds and dwell times affected the strength of AA5052-H112 aluminium alloy sheets welded by the FSSW method. Their findings revealed that while dwell time had an impact on joint strength, increasing the rotational speed led to a reduction in strength. Uğurlu and Çakan [28] examined the FSSW of AA7075-T6 spot joints with a constant dwell time of 20 s and different tool rotation speeds. They found that higher tool rotational speeds enhanced joint properties, with the highest joint strength achieved in joints processed at the maximum rotational speed, provided they were defect-free [29].

Despite their industrial significance, limited research has investigated the impact of FSSW parameters, particularly dwell time, on the mechanical performance of AA6061–AA7075 spot joints. This study aims to bridge this gap by analyzing how dwell time influences the microstructure and lap shear strength of these dissimilar joints, providing valuable insights for optimizing FSSW in advanced engineering applications.

2. Experimental procedure

This study employed AA6061 and AA7075 alloy sheets as base materials, each measuring 100 mm × 35 mm with a thickness of 2 mm. The chemical composition of these alloy sheets is detailed in Table 1.

AA6061-AA7075 strips, measuring 100×35 mm, were prepared using the Wire electrical discharge machining process for these experiments. An H13 steel tool, specifically customised for this experiment, featured a tool pin length of 2.85 mm and a cylindrical shoulder diameter of 5 mm as shown in Figure 1a. This tool underwent heat treatment to attain a hardness of 52–55 HRC, ensuring its durability and wear resistance during the friction stir welding process [2, 16]. In this study, the FSSW process was conducted using a CNC vertical machining centre, equipped with a specially designed fixture for clamping the overlapped specimens, as shown in Figures 1b and 1c.

The FSSW process involved three main stages: plunging, dwelling, and retraction. During the plunging stage, the rotating tool was pressed into the overlapping aluminium alloy sheets, generating frictional heat. The dwell time, defined as the duration for which the tool remained stationary while maintaining rotational motion at a constant speed, was a critical parameter in this study. Dwell times of 2, 4, 6, and 8 s were implemented to analyze their effects on joint quality. During the dwell phase, the tool's rotation and the applied axial force facilitated material stirring and bonding at the interface. Finally, in the retraction stage, the tool was withdrawn vertically, leaving behind a circular spot weld. Additional process parameters included a tilt angle of 0°, plunge depth of 3.2 mm, and plunge rate of 0.1 mm/sec. These parameter settings were derived from trial experiments and studies on the selected materials [30–33].

The specimens were polished using SiC abrasive papers and alumina paste, followed by etching with Keller's reagent to reveal the

Table 1. The chemical composition of the base material (in wt.%).

Elements	Zn	Fe	Ti	Si	Mg	Cr	Mn	Cu	Al
AA6061	0.200	0.25	0.02	0.13	2.49	0.19	0.09	0.001	Bal.
AA7075	6.20	0.10	0.05	0.4	2.00	0.19	0.05	1.70	Bal.

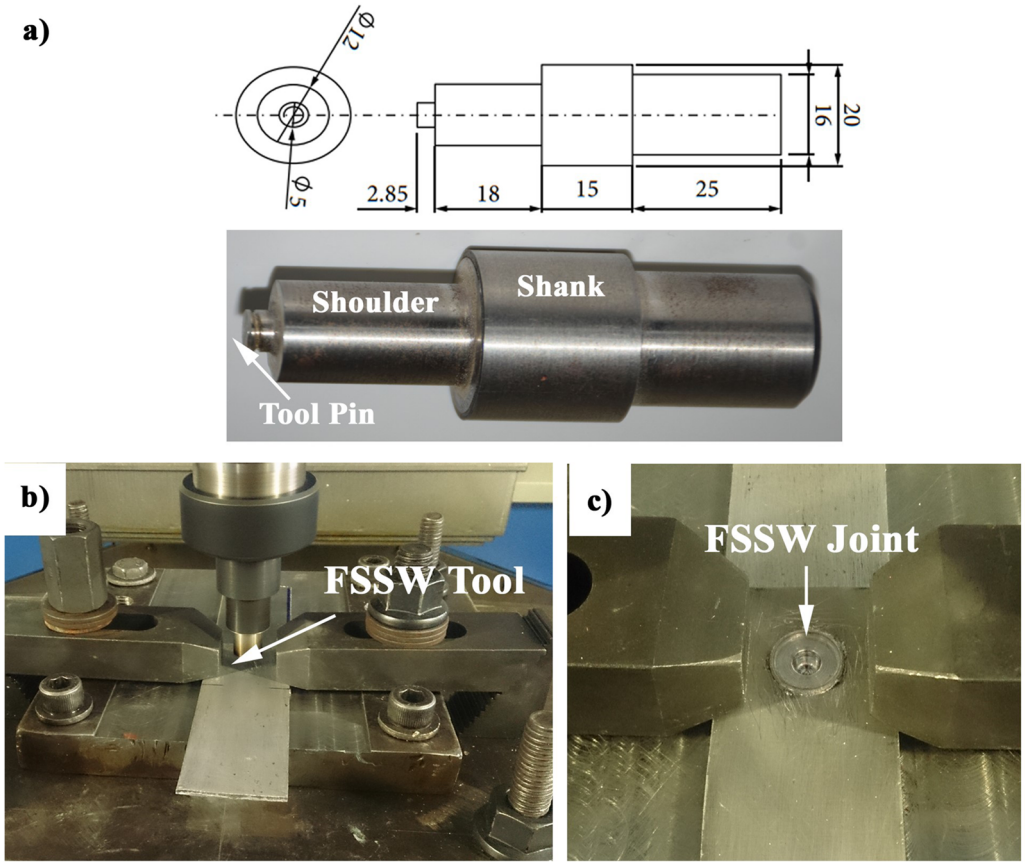

Figure 1. (a) Schematic drawing and image showing the FSSW tool (dimensions in mm), and (b–c) FSSW experimental set-up.

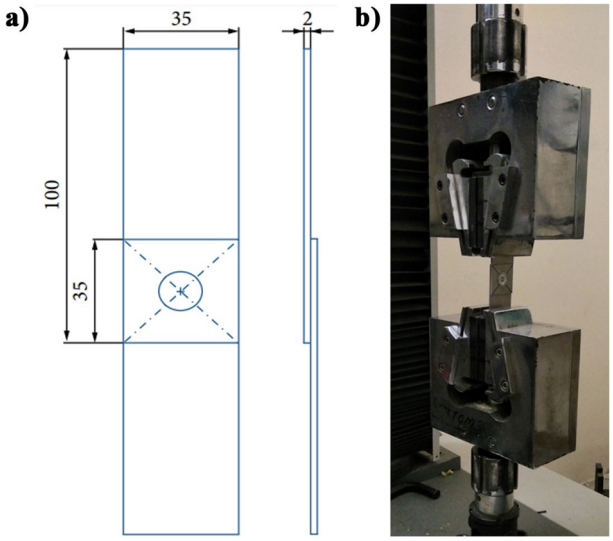

Figure 2. (a) Drawing showing the tensile–shear test specimen (dimensions in mm), and (b) photographic image of the specimen during the tensile-shear test.

microstructure. Microstructural analysis was performed using an optical microscope and a Field Emission Scanning Electron Microscope (FESEM). Mechanical performance was assessed through lap shear tensile tests conducted at room temperature, with each condition tested using at least three specimens. A universal testing machine with a crosshead speed of 0.05 mm/sec was used to measure the lap shear strength. The dimensions of the tensile–shear test specimens are illustrated in Figure 2a, while Figure 2b shows a photographic image of the specimen during the test. The applied load and displacement were recorded continuously to evaluate the joint strength and fracture behavior.

3. Results and discussion

3.1. Joint appearance

Figure 3 displays the surface characteristics of the FSSW joints produced at various dwell times. A visible keyhole and circular shoulder indentation, common features of FSSW joints, were observed for all welding conditions. As the dwell duration grows during the FSSW process, the temperature also rises, reducing the viscosity of the substance being stirred. A slight flash formed at the highest dwell time, indicating excessive heat and material displacement. This keyhole reflects the pin's geometry and dimensions, and the light intensity increases with the rise in dwell because of the improved softening of the material surrounding the rotating pin.

As the dwell time increased from 2 to 8 s, the temperature rise softened the materials, resulting

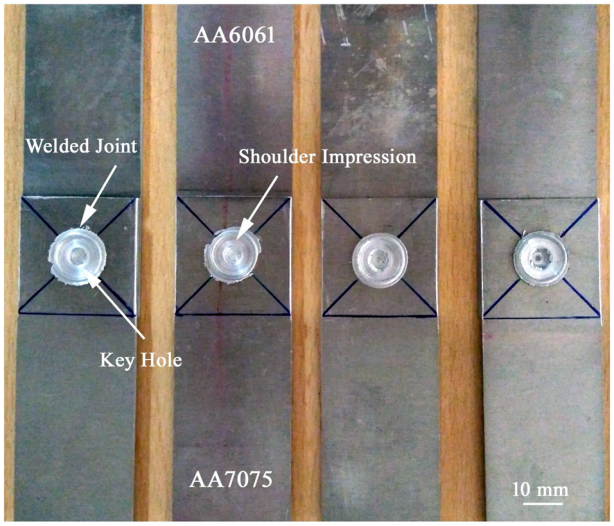

Figure 3. Appearance of the AA6061-AA7075 FSSW joints fabricated at different dwell times.

in deeper shoulder impressions, as shown in Figure 3. The shoulder impressions for varying dwell times are visible in Figure 3, providing a qualitative representation of the tool's interaction with the surface. For a quantitative analysis, the average diameter of the shoulder impression was measured for each weld. The results showed dimensions of approximately 5.0 mm for a 2-second dwell, 5.2 mm for 4 s, 5.6 mm for 6 s, and 5.8 mm for 8 s. These measurements demonstrate the relationship between dwell time and the extent of material deformation caused by the tool shoulder. Additionally, the uniformity of the impressions was evaluated to assess the consistency of heat input. It was observed that larger and deeper impressions at longer dwell times corresponded to excessive heat input, which potentially affected the grain structure and reduced joint integrity.

A deviation in the cross-sectional macrostructure of FSSW AA6061-AA7075 joints is evident as the dwell ranges from 2 to 8 s, as shown in Figure 4. The stir zone (SZ) morphology associated with each cross-section changes significantly with dwell time. The weld processed with a 6-second dwell time exhibited the largest stir zone, showing optimal material flow and heat input, as illustrated in Figure 4. Increasing the dwell time expanded the SZ width (SW), particularly around the keyhole, demonstrating the strong influence of heat generation on joint formation. The analysis demonstrates that dwell time plays a critical role in enlarging the weld area surrounding the keyhole. The micrographs confirmed that longer dwell times enabled effective plasticization and smooth bonding between the two alloys, with no visible voids or

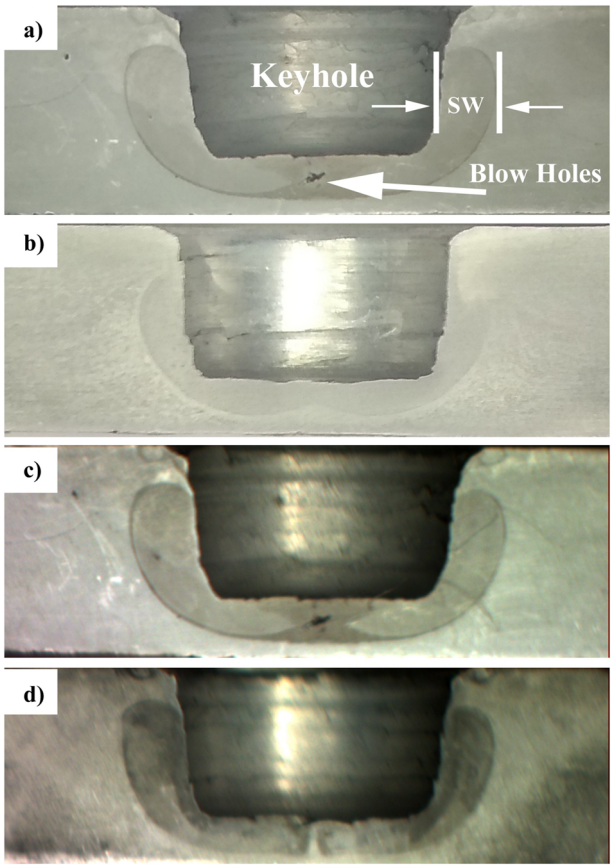

Figure 4. Cross-sectional macrographs showing the FSSW joint processed at different dwell times of (a) 2 Sec, (b) 4 Sec, (c) 6 Sec and (d) 8 Sec.

cracks in the weld area. The formation of a defect-free weld zone is predominantly governed by the amount of plasticized material generated and the consistency of material movement through the welding process. Adequate plasticization ensures the proper fusion of materials within the SZ, resulting in sound mechanical properties.

Based on these observations, it is evident that the selected set of process parameters, including the dwell time, is sufficient for fabricating high-quality AA6061-AA7075 spot joints. The optimized parameters, particularly the 6-second dwell time, allow for proper heat generation and material flow, producing a well-refined SZ and ensuring the structural integrity of the weld.

3.2. Influence of the dwell time on the lap shear fracture load

Figure 5 illustrates the effect of dwell time on lap shear fracture load. The highest tensile load of 5925 N was achieved with a 6-second dwell time, indicating an optimal balance of heat input and material flow. It can be detected that the fracture load increases with a dwell time of up

to 6 s, suggesting that this time frame allows for sufficient heat input to promote plastic deformation and effective interfacial bonding between the materials. Shorter dwell times (2–4 s) generated insufficient heat, resulting in weak interfacial bonding and lower fracture loads. As dwell time increased, enhanced plastic deformation improved joint strength up to 6 s. However, beyond this point, the lap shear strength declined due to excessive grain growth and thermal stress, weakening the weld integrity [34].

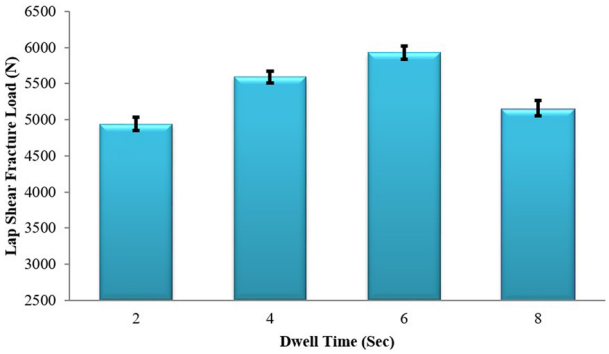

Figure 5. Lap shear fracture load test result.

Additionally, over-stirring of the material during longer dwell times can cause a degradation in the material properties at the weld interface due to potential void formation, increased thermal stresses, or the dissolution of strengthening precipitates [35]. This results in reduced joint integrity. The observed decrease in strength at higher dwell times is likely due to a combination of excessive grain growth and poor material flow, which compromises the mechanical interlocking at the weld interface.

3.3. Effect of dwell time on failure pattern

Figure 6 displays various views of the lap shear-tested specimens under different dwell conditions. To better understand the shear

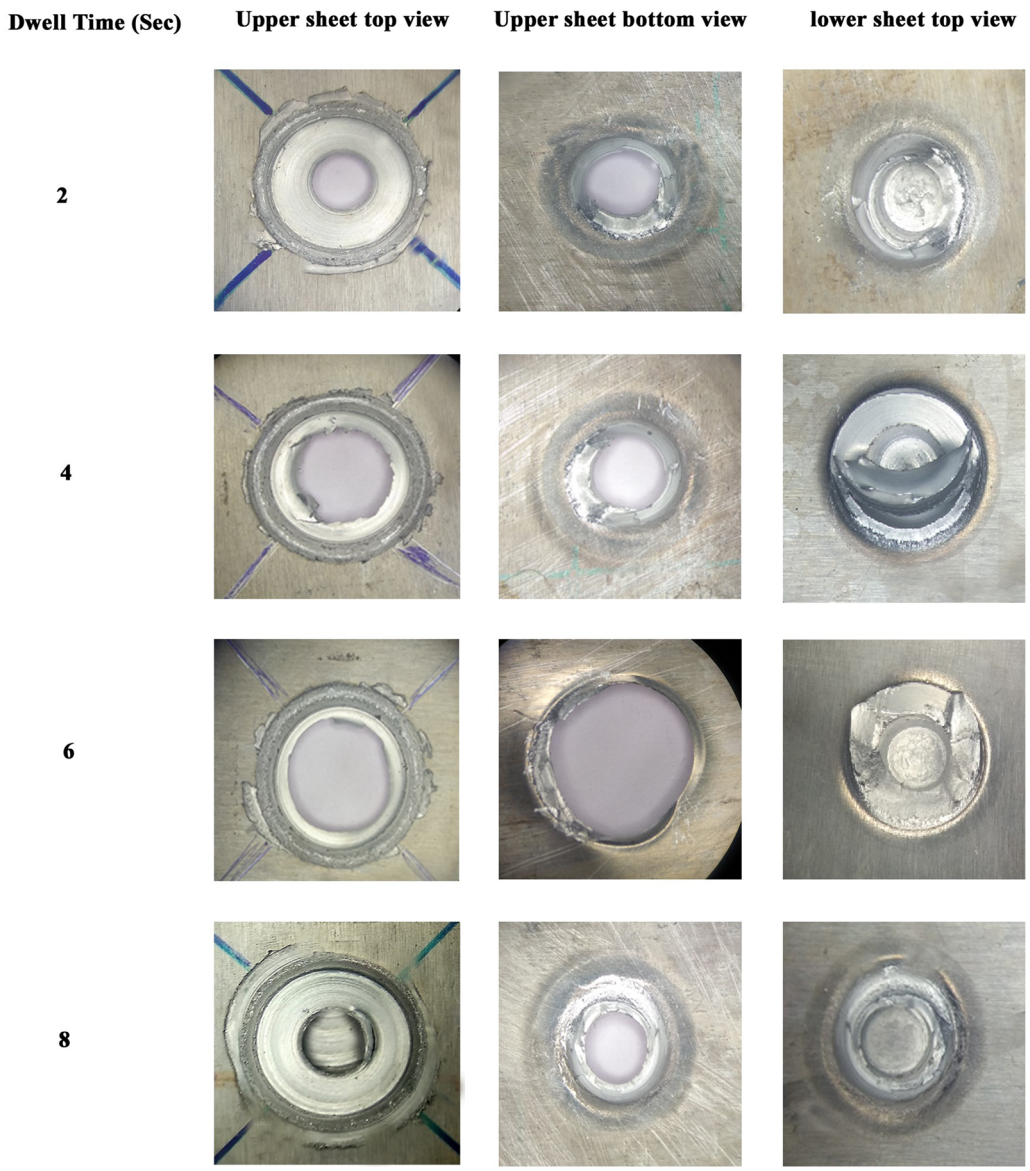

Figure 6. Fracture surfaces of lap shear tested specimens.

fracture mechanism in the lap section, the fracture surfaces of the samples were carefully examined post-lap shear testing. In samples with lower strength, cracks were observed to initiate in the partially bonded regions due to multiple nucleation sites, with the cracks propagating across the bonded area.

This fracture behaviour was particularly evident in the welds produced with 2 and 8 s of dwell time, leading to reduced lap shear tensile strength. In contrast, the specimen welded with a dwell time of 6 s exhibited shear-off around the circumference of the keyhole, resulting in higher lap shear tensile strength. This outcome aligns with the findings reported in [36], where tearing along the keyhole circumference contributed to improved mechanical performance.

The broken lower sheet of the lap shear specimens exposed to 6 and 8 s of dwell time, respectively, is shown in FESEM pictures in Figures 7 and 8. The micrographs reveal distinct differences in the fracture surface morphology, reflecting the mechanical performance under varying welding conditions. In the weld with a 6-second dwell time (Figure 7), the fracture surface exhibits a fine distribution of dimples, indicative of a ductile fracture mechanism.

The significant elongation observed is by the superior joint strength at this dwell time, suggesting that the optimal balance between heat input and material flow was achieved, allowing for effective plastic deformation and crack resistance [37]. In contrast, the fracture surface of the specimen with an 8-second dwell time (Figure 8) displays a markedly different morphology. While dimples are still present, large pores are also visible across the fracture plane, indicating localized void formation. These pores suggest that excessive heat input during the prolonged dwell time may have caused degradation in the microstructure, leading to porosity and reduced joint strength. The

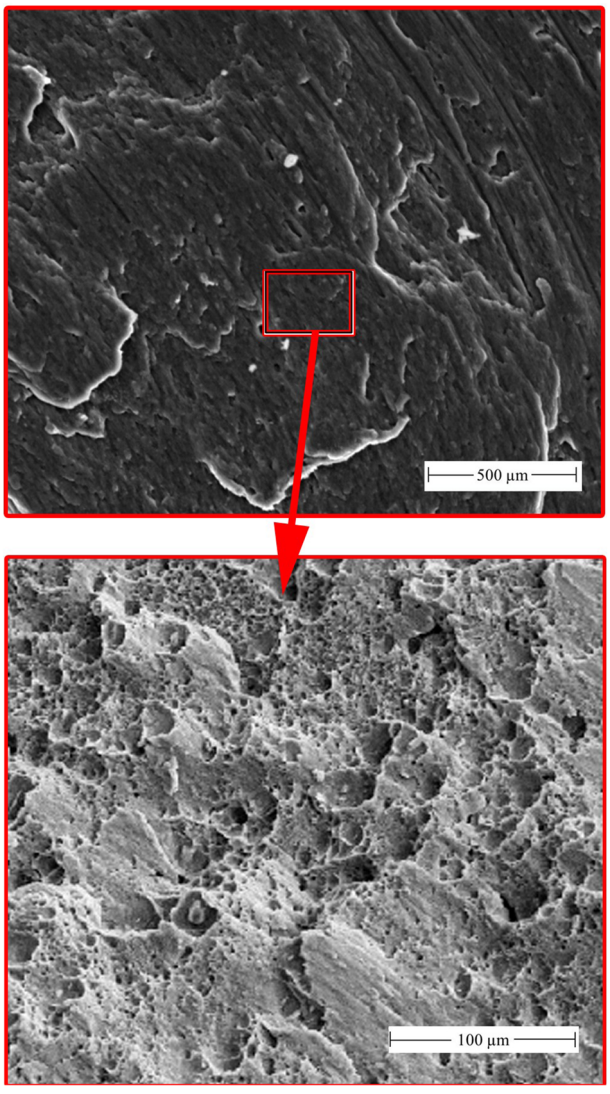

Figure 7. SEM Images showing the fracture surfaces of the failed joint the joint FSSWed at 6-second dwell time.

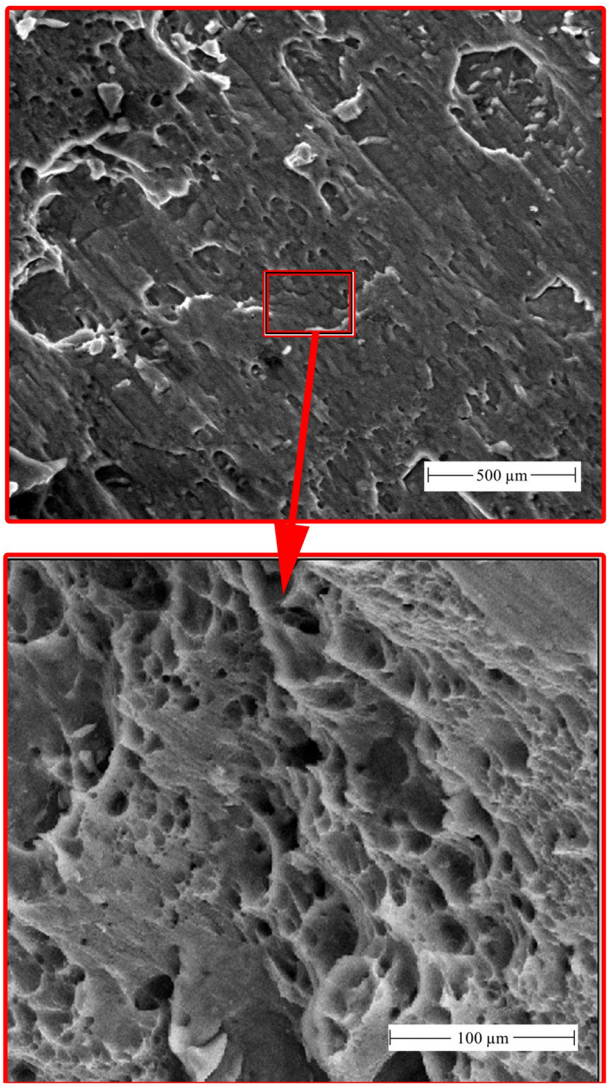

Figure 8. SEM Images showing the fracture surfaces of the failed joint the joint FSSWed at 8-second dwell time.

coarser dimples and voids are consistent with a loss of ductility and indicate a transition towards a brittle fracture mechanism [38, 39]. Additionally, the stretched-out dimples in the same direction point to a shear fracture mode, likely due to material tearing under the applied load. This supports the observation that excessive heat during the 8-second dwell time led to a decline in weld quality, as reflected in the lower lap shear fracture load.

4. Conclusion

This study highlights the critical influence of dwell time on the microstructure and mechanical properties of FSSW dissimilar AA6061–AA7075 joints. The following conclusions can be drawn:

- A dwell time of 6 seconds yielded the highest lap shear strength of 5925 N, demonstrating that an optimal balance between heat input, material flow, and microstructural stability is crucial for achieving superior joint strength.
- Shorter dwell times (2–4 seconds) resulted in inadequate heat input, leading to poor plasticization and weak bonding, while prolonged dwell times (8 seconds) caused excessive heat, grain coarsening, and void formation, compromising joint strength.
- Microstructural analysis of fracture surfaces revealed that the 6-second dwell time produced a ductile fracture mode, with fine dimples indicating enhanced plastic deformation and crack resistance. In contrast, the 8-second dwell time led to the formation of pores and coarser dimples, suggesting a shift toward brittle fracture and reduced joint performance.

Disclosure statement

No potential conflict of interest was reported by the authors.

Ethics statement

Not applicable as none of any human participants or animals are involved in the study.

Consent for publication

All the authors have read and given their consent to submit the manuscript for the peer review process in the journal for possible publication.

Funding

Suresh S gratefully acknowledges the financial support from the Science and Engineering Research Board (SERB) under grant SSY/2023/001464. This support was instrumental in facilitating discussions and knowledge exchange that significantly contributed to the development of this paper.

Data availability statement

All the experimental and analyzed data in this study are reported in this article itself.

References

[1] Suresh S, Venkatesan K, Natarajan E. Influence of SiC nanoparticle reinforcement on FSS Welded 6061-T6 aluminum alloy. J Nanomater. 2018;2018:1–11. doi: 10.1155/2018/7031867

[2] Suresh S, Venkatesan K, Natarajan E, et al. Influence of tool rotational speed on the properties of friction stir spot welded AA7075-T6/Al2O3 composite joint. Mater Today Proc. 2020;27:62–67. doi: 10.1016/j.matpr.2019.08.220

[3] Guo JF, Chen HC, Sun CN, et al. Friction stir welding of dissimilar materials between AA6061 and AA7075 Al alloys effects of process parameters. Mater Des. 2014;56:185–192. doi: 10.1016/j.matdes.2013.10.082

[4] Raturi M, Garg A, Bhattacharya A. Joint strength and failure studies of dissimilar AA6061-AA7075 friction stir welds: effects of tool pin, process parameters and preheating. Eng Fail Anal. 2019;96:570–588. doi: 10.1016/j.engfailanal.2018.12.003

[5] Subramani V, Jayavel B, Sengottuvelu R, et al. Assessment of microstructure and mechanical properties of stir zone seam of friction stir welded magnesium AZ31B through nano-SiC. Materials (Basel). 2019;12(7):1044. doi: 10.3390/ma12071044

[6] Xiao R, Zhang X. Problems and issues in laser beam welding of aluminum–lithium alloys. J Manuf Process. 2014;16(2):166–175. doi: 10.1016/j.jmapro.2013.10.005

[7] Doshi SJ, V Gohil A, Mehta ND, et al. Challenges in Fusion Welding of Al alloy for Body in White. Mater Today Proc. 2018;5(2):6370–6375. doi: 10.1016/j.matpr.2017.12.247

[8] Shete M, Yarasu R, Sonar T, et al. Improving friction stir spot welding of high-density polyethylene sheets for welding parameters and its optimization. Int J Interact Des Manuf. 2024;18(7):4513–4525. doi: 10.1007/s12008-023-01720-y

[9] El-Sayed MM, Shash AY, Abd-Rabou M, et al. Welding and processing of metallic materials by using friction stir technique: a review. J Adv Join Process. 2021;3:100059. doi: 10.1016/j.jajp.2021.100059

[10] Yang XW, Fu T, Li WY. Friction stir spot welding: a review on joint macro-and microstructure, property, and process modelling. Adv. Mater. Sci. Eng. 2014;2014:1–11. vol. doi: 10.1155/2014/697170

[11] Suresh S, Natarajan E, Mohan DG, et al. Depriving friction stir weld defects in dissimilar aluminum lap joints.

Proc Inst Mech Eng Part E J Process Mech Eng. 2024:9544089241239817. doi: 10.1177/09544089241239817
[12] Sukkasamy S, Gopal PM. Monitoring of the friction stir welding process: Upgrading towards industry 4.0. In Thanigaivelan R, Rajan N, Argul T, editors. Advanced manufacturing techniques for engineering and engineered materials. IGI Global Scientific Publishing; 2022. p. 173–182. doi: 10.4018/978-1-7998-9574-9.ch010
[13] Venukumar S, Baby B, Muthukumaran S, et al. Microstructural and mechanical properties of walking friction stir spot welded AA 6061-T6 sheets. Procedia Mater Sci. 2014;6:656–665. doi: 10.1016/j.mspro.2014.07.081
[14] Suresh S, Natarajan E, Vinayagamurthi P, et al. Optimum tool traverse speed resulting equiaxed recrystallized grains and high mechanical strength at swept friction stir spot welded AA7075-T6 lap joints. Natarajan E. Vinodh S. Rajkumar V. Materials, Design and Manufacturing for Sustainable Environment (pp. 547–555). Singapore: Springer Nature Singapore; 2023. doi: 10.1007/978-981-19-3053-9_41
[15] Suresh S, Venkatesan K, Natarajan E, et al. Evaluating weld properties of conventional and swept friction stir spot welded 6061-T6 aluminium alloy. Mat Express. 2019;9(8):851–860. doi: 10.1166/mex.2019.1584
[16] Suresh S, Venkatesan K, Rajesh S. In *AIP Conference Proceedings*. Optimization of process parameters for friction stir spot welding of AA6061/Al2O3 by Taguchi method, p. 30018; 2019. doi: 10.1063/1.5117961
[17] Yang Q, Mironov S, Sato YS, et al. Material flow during friction stir spot welding. Mater. Sci. Eng. A. 2010;527(16-17):4389–4398. doi: 10.1016/j.msea.2010.03.082
[18] Pan T-Y. *SAE World Congress & Exhibition*. Friction Stir Spot Welding (FSSW) - a Literature Review. SAE International; 2007. doi: 10.4271/2007-01-1702
[19] Nathan SR, Rajendran C, Sonar T, et al. Optimization of CNC-FSSW parameters for dissimilar spot welding of AA6061 aluminium alloy and mild steel using Taguchi based desirability function approach. Int J Interact Des Manuf. 2025;19(1):337–346. doi: 10.1007/s12008-023-01728-4
[20] Rajendran C, Sonar T, Ivanov M, et al. Mathematical modeling, optimization and prediction of friction stir spot welding parameters for dissimilar joining AA2024-T6 aluminium and AZ31B magnesium alloy in lap weld configuration. Int J Interact Des Manuf. 2025;19(1):275–289. doi: 10.1007/s12008-023-01669-y
[21] Nagarajan BM, Manoharan M. Enhancement of joint strength of dissimilar aluminum/polymer hybrid joints by friction stir spot welding by surface textures. J Adhes Sci Technol. 2024;38(8):1284–1311. doi: 10.1080/01694243.2023.2256557
[22] Çam G, Javaheri V, Heidarzadeh A. Advances in FSW and FSSW of dissimilar Al-alloy plates. J Adhes Sci Technol. 2023;37(2):162–194. doi: 10.1080/01694243.2022.2028073
[23] Kalagara S, Muci-Kuchler KH, Arbegast W. Visualization of material flow in a refill friction stir spot welding process using marker materials. SAE Int J Mater Manuf. 2010;3(1):628–651. doi: 10.4271/2010-01-0971
[24] Buffa G, Fratini L, Piacentini M. On the influence of tool path in friction stir spot welding of aluminum alloys. J Mater Process Technol. 2008;208(1–3):309–317. doi: 10.1016/j.jmatprotec.2008.01.001
[25] Jayabalakrishnan D, Balasubramanian M. Friction stir weave welding (FSWW) of AA6061 aluminium alloy with a novel tool-path pattern. Aust J Mech Eng. 2019;17(2):133–144. doi: 10.1080/14484846.2017.1373584
[26] Choi D-H, Ahn B-W, Lee C-Y, et al. Formation of intermetallic compounds in Al and Mg alloy interface during friction stir spot welding. Intermetallics. 2011;19(2):125–130. doi: 10.1016/j.intermet.2010.08.030
[27] Zhang Z, Yang X, Zhang J, et al. Effect of welding parameters on microstructure and mechanical properties of friction stir spot welded 5052 aluminum alloy. Mater Des. 2011;32(8-9):4461–4470. doi: 10.1016/j.matdes.2011.03.058
[28] Uğurlu M, Çakan A. The effect of tool rotation speed on mechanical properties of friction stir spot welded (FSSW) AA7075-T6 aluminium alloy sheets. Eur Mech Sci. 2019;3(3):97–101. doi: 10.26701/ems.520139
[29] Suresh S, Natarajan E, Shanmugam R, Venkatesan K, Saravanakumar N ,AntoDilip A. Strategized friction stir welded AA6061-T6/SiC composite lap joint suitable for sheet metal applications. J Mater Res Technol. 2022;21:30–39. doi: 10.1016/j.jmrt.2022.09.022
[30] Suresh S, Elango N, Venkatesan K, et al. Sustainable friction stir spot welding of 6061-T6 aluminium alloy using improved non-dominated sorting teaching learning algorithm. J. Mater. Res. Technol. 2020;9(5):11650–11674. doi: 10.1016/j.jmrt.2020.08.043
[31] Suresh S, Natarajan E, Franz G, et al. Differentiation in the SiC filler size effect in the mechanical and tribological properties of friction-spot-welded AA5083-H116 alloy. Fibers. 2022;10(12):109. doi: 10.3390/fib10120109
[32] Suresh S, Velmurugan D, Balaji J, et al. Influences of nanoparticles in friction stir welding processes. Sustainable Utilization of Nanoparticles and Nanofluids in Engineering Applications (pp. 32–55). Hershey, PA: IGI Global; 2023. doi: 10.4018/978-1-6684-9135-5.ch002
[33] Suresh S, Premnath P, Balaji C, et al. Friction stir welding: a comprehensive review of non-metallic particle reinforcement in joints. J Mater Eng. 2024;2(3):207–219. doi: 10.61552/JME.2024.03.006
[34] Ahmed MMZ, El-Sayed Seleman MM, Albaijan I, El-Aty AA. Microstructure, texture, and mechanical properties of friction stir spot-welded AA5052-H32: influence of tool rotation rate. Materials (Basel). 2023;16(9):3423. doi: 10.3390/ma16093423
[35] Xie X, Shen J, Gong F, et al. Effects of dwell time on the microstructures and mechanical properties of water bath friction stir spot-welded AZ31 magnesium alloy joints. Int J Adv Manuf Technol. 2016;82(1-4):75–83. doi: 10.1007/s00170-015-7361-2
[36] Liao H, Chen J, Peng L, et al. Fabrication and characterization of magnesium matrix composite processed by combination of friction stir processing and high-energy ball milling. Mater Sci Eng A. 2017;683:207–214. doi: 10.1016/j.msea.2016.11.104
[37] Gopal PM, Kavimani V. Influence of silica rich CRT and BN on mechanical, wear and corrosion character-

istics of copper-surface composite processed through friction stir processing. Silicon. 2021;13(10):3431–3440. doi: 10.1007/s12633-020-00764-z

[38] Suresh S, Venkatesan K, Natarajan E, et al. Performance analysis of nano silicon carbide reinforced swept friction stir spot weld joint in AA6061-T6 alloy. Silicon. 2021;13(10):3399–3412. doi: 10.1007/s12633-020-00751-4

[39] Sudhagar S, Gopal PM. Investigation on mechanical and tribological characteristics Cu/Si3N4 surface composite developed through friction stir processing. Silicon. 2022;14(8):4207–4216. doi: 10.1007/s12633-021-01206-0